Polarized-cathodoluminescence study of stress for GaAs grown selectively on patterned Si(100)

Y. Tang and D. H. Rich[a)]
Photonic Materials and Devices Laboratory, Department of Materials Science and Engineering,
University of Southern California, Los Angeles, California 90089-0241

E. H. Lingunis and N. M. Haegel
Department of Materials Science and Engineering, University of California, Los Angeles, California 90024

The spatial variation of stress tensor in selective-area metalorganic chemical-vapor-deposition-grown GaAs on Si substrate by using a linearly polarized cathodoluminescence (CL) technique has been examined. The polarized CL technique enables a precise determination of the energy positions for the strain-split $j = 3/2$ valence-band excitonic contributions to the luminescence by a simultaneous deconvolution of two CL spectra that are each taken under different polarization detection conditions; this procedure enables a mapping of the stress tensor. The biaxial in-plane stress ($\sigma_\parallel = \sigma_\perp$; where $\parallel$ and $\perp$ denote parallel and perpendicular, respectively, to a $\langle 110 \rangle$-oriented mesa edge) is found to decrease from ~ 2.2 to 0.5 kbar as the square pattern size is decreased from 1 mm to 10 μm. Patterns having smaller dimension are found to have an increased luminescence efficiency, indicating a reduction in thermal stress induced dislocation density. The stress decay in the vicinity of edges and corners is found to be modeled well with a bimetal thin-film model, showing an approximately exponential decay in stress. A residual tensile stress (comprised of nonzero $\sigma_\perp$, shear and peeling stress terms) of 0.5–1.0 kbar is found to exist at the edges and corners of the square GaAs mesas; this result agrees qualitatively with an elastic finite-element analysis. The CL results show that the decay length of stress relief near a pattern edge essentially increases with increasing mesa size. The maximum biaxial stress and residual stress near the mesa edges and corners is found to increase with increasing pattern size. Polarized CL imaging is observed to be sensitive to local deviations from biaxial stress and can be used to map the boundaries of stress contours near mesa edges and defects.

I. INTRODUCTION

Heteroepitaxial GaAs films grown on Si substrate have attracted a great deal of attention in recent years, owing to the possibilities for monolithic integration of electronic and photonic technologies.[1-10] High-quality heteroepitaxial GaAs/Si growth offers the opportunity of combining the high reliability and accessibility of Si-based microelectronics processing with the high-speed and light-emitting capabilities of GaAs and other III-V alloys; however, such applications are not without some serious material-related problems inhibiting high-quality growth. A 4.2% lattice mismatch between GaAs and Si at growth temperature is compensated by dislocations at the interface. Also, since the ratio of the GaAs and Si thermal-expansion coefficients is about 2.5 at typical growth temperatures in excess of 700 °C, the subsequent cooling to room temperatures results in a large tetragonal distortion which can cause wafer bowing and the formation of microcracks to partially relieve the thermal stress. The residual thermal stress and distribution of microcracking on GaAs/Si will alter the electronic and optical properties, and the effects of stress on the splitting of the $j = 3/2$ heavy-hole (hh; $m_j = \pm 3/2$) and light-hole (lh; $m_j = \pm 1/2$) bands at $\mathbf{k} = 0$ have been studied, and optical transitions involving these states exhibit polarization selection rules which depend on the strain.[11,12] Recently, we have demonstrated that polar-

ized cathodoluminescence (CL) imaging and spectroscopy can be a useful tool to study the stress-induced splitting of the $j = 3/2$ valence bands.[1] In order to more fully understand the ramifications associated with fabricating devices with the GaAs/Si system, it is essential to elucidate in detail the spatial variation in the strain, and a high-spatial resolution technique, such as offered in CL, is needed to locally probe the strain-induced splitting of the $j = 3/2$ valence bands. The GaAs/Si system has been studied using photoluminescence (PL),[2-5] photoluminescence excitation (PLE),[6] photoreflectance (PR),[7,8] and CL.[1,9,10]

In order to minimize the presence of microcracks and reduce the dislocation density in GaAs films grown on Si, the selective growth of GaAs on reduced substrate areas formed by patterning is employed. In this article we present the results of a polarized CL experiment used to study the effect of pattern size on the spatial variation in stress tensor near the edge and the corner of square-shaped GaAs patterns selectively grown on a Si substrate for various square sizes using metalorganic chemical-vapor deposition (MOCVD). Polarized CL imaging is used to distinguish between regions of biaxial tensile stress and uniaxial tensile stress. The imaging shows clearly how structural defects in the form of microcracks and pattern edge effects can lead to uniaxial stress. Using polarized CL spectroscopy, the decomposition of the luminescence spectral line shape into the two distinct strain-split $j = 3/2$ components can be accomplished by utilizing

the polarization dependence of the hh and lh wave functions. In order to obtain the stress tensor components from the luminescence spectra, the positions of the strain-split $j=3/2$ peaks derived from the excitonic luminescence must be measured accurately, and we show that a precise deconvolution is facilitated by polarization spectroscopy.[1] The CL measurements here are used to measure fundamental parameters associated with the selective-area growth, such as the length of the transition region from biaxial stress to uniaxial stress near a mesa edge, the maximum biaxial stress present on a mesa, the residual tensile stress remaining at the edge of the mesa, the mesa size at which microcracking begins, and the optical quality of the film as a function of pattern size. In this article we analyze quantitatively the relative contributions of stress perpendicular to the mesa edge, shear and peeling stress terms to the total residual stress remaining at the mesa edges. A theoretical finite-element (FE) analysis is also employed to study the residual stresses remaining at the mesa edges. The ability to ultimately optimize III-V devices fabricated on Si is linked to a better understanding of these stress parameters.

II. EXPERIMENT

A. Sample preparation

The sample studied was grown at Spire Corporation in a MOCVD reactor with modification for atomic layer epitaxy (ALE) operation using trimethylgallium (TMG) and arsine (AsH₃).[3] For selective growth, 2 in., n-type Si wafers oriented 2° off the (001) towards the [110] direction were initially covered with SiO₂ to a thickness 0.5–0.6 μm. Using such vicinal Si(001) substrates, the amount of antiphase disorder in the resulting GaAs film is markedly reduced due to the increased biatomic step density on the vicinal Si surface.[13] Squares with dimensions in the range 10–1000 μm with their edges parallel to the two orthogonal ⟨110⟩ directions were photolithographically defined on a SiO₂ mask and windows were etched down to the Si substrate. Following an initial high-temperature bakeout in H₂, a 100–200 Å nucleation layer was deposited by ALE. Conventional growth was then resumed at 650 °C until the thickness of GaAs layer reached 1 μm. Finally, the SiO₂ mask was removed by etching in 5% buffered HF and, after which, only GaAs square mesas remained on the Si substrate.

B. Linearly polarized cathodoluminescence system

A JEOL 840A scanning electron microscope (SEM) was modified for linearly polarized CL measurements. The CL optical collection system and cryogenic specimen stage were designed and constructed at USC.[1] The luminescence emitted from the sample was collected with an ellipsoidal mirror which focuses the radiation onto a coherent optical fiber bundle leading outside the SEM vacuum chamber to a 0.25 m focal length monochromator. The coherency of the bundle allows for a direct imaging of light at the second ellipsoidal focus into the entrance slit of the monochromator. The bundle acts as an efficient polarization scrambler, and to perform polarization measurements a rotatable vacuum polarizer was mounted directly in front of the bundle. In order to
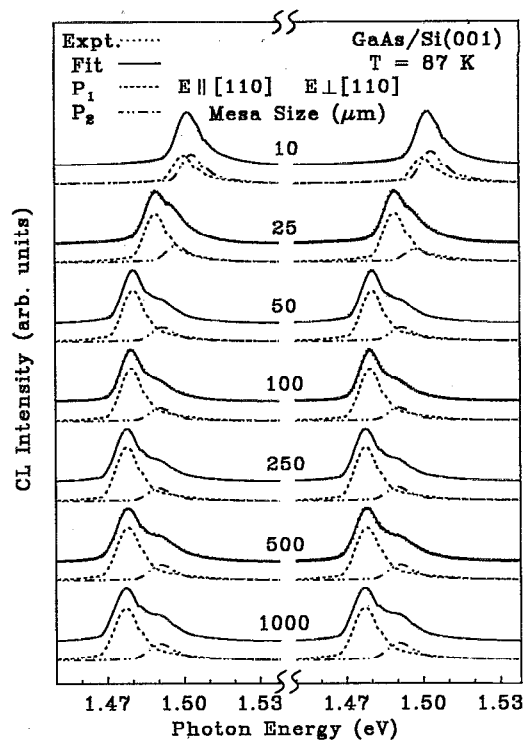

FIG. 1. Local cathodoluminescence spectra taken at the centers of square mesas of GaAs on Si. Mesa sizes are indicated in the figure. The decomposition of the luminescence line shape into two components (labeled as P_1 and P_2) resulting from the strain-induced splitting of the top valence bands is shown. The overall fit to the data is indicated by a solid line running through the data.

account for polarization mixing effects caused by reflection at the mirror, e.g., due to finite solid angle of collection and changes in the electric field $\mathbf{E}$, phase, and amplitude, a linearly polarized Lambertian (cosine) source was placed at the focus to simulate emission from the sample and to correct reflection-induced changes in polarization. For CL measurements, A 30 keV electron probe was used with a probe current of approximately 5 nA. The light emitted from the sample, dispersed by a $\frac{1}{4}$ m monochromator with spectral resolution of 2 nm, was detected by a cooled Cs:GaAs photomultipier tube (PMT). Local CL spectra for the polarized emissions were taken with polarization directions set parallel to the edges of the square-patterned mesa. The spectra were analyzed to yield the energies and intensities of strain-split hh and lh excitonic transitions by simultaneously fitting both spectra for two polarization directions. The temperature of the cryogenic sample stage is continuously tunable from ~15 to 350 K, and temperatures ranged from 87 to 150 K in this study.

III. RESULTS AND DISCUSSION

A. Effect of pattern size on biaxial stress

We have examined the effect of pattern size on the biaxial stress. Polarized CL spectra were taken with the electron beam fixed at the center of the square-patterned mesa for various mesa sizes as shown in Fig. 1. The spectra were taken with the polarizer set to detect emission for E⊥[110]
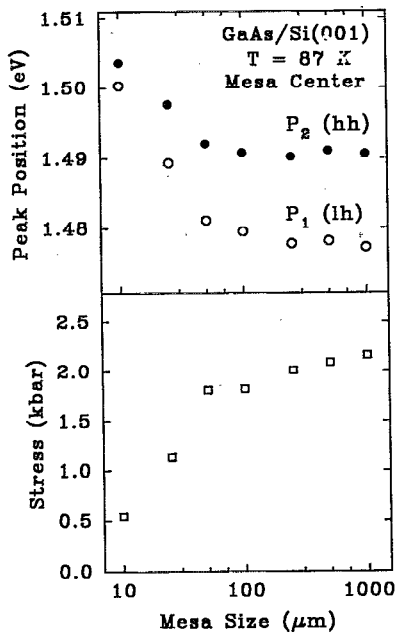
FIG. 2. Results of the fits of Fig. 1 showing the energy positions of P_1 and P_2 and the biaxial stress calculated from Eq. (3), both as a function of mesa size.
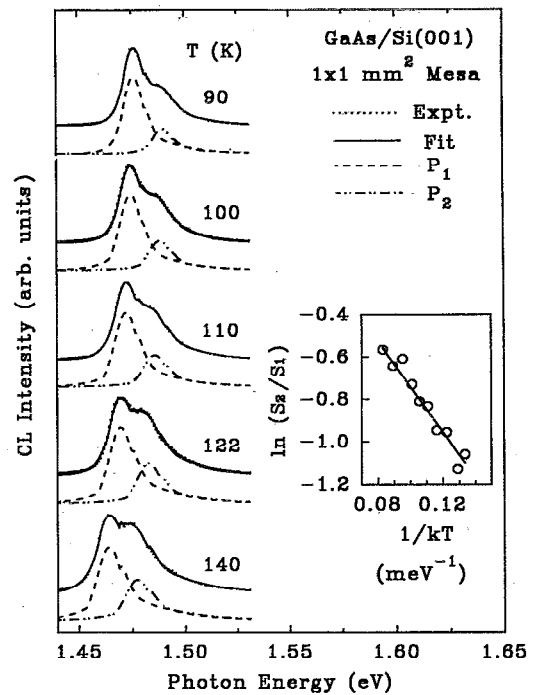

FIG. 3. Local CL spectra for the 1 mm mesa for various temperatures. The ratio of the integrated intensities of peaks P_1 and P_2 is shown as a function of $1/kT$ in the inset.

and $E \parallel [110]$, where the mesa edges are aligned with respect to the $\langle 110 \rangle$ directions. A distinct peak with a single shoulder at higher photon energies is observed in all the CL spectra of Fig. 1. These two peaks can be decomposed into two excitonic transition features resulting from the strain-induced splitting of the $j = 3/2$ valence bands. The model for the decomposition and the fitting procedure has been previously described.[1] This model includes parameters that describe excitonic linewidth, higher-energy band-to-band transitions, inhomogeneous broadening, and thermal broadening.[1] From the fits, the intensity and energy position of each component can be determined. The results of the fits are indicated by the solid lines running through the data points and the decomposed strain split components, labeled P_1 and P_2, are shown offset below the spectra. The spectra of Fig. 1 show that the line shape is insensitive to the polarizer orientation, as the detected emissions with $E \perp [110]$ and $E \parallel [110]$ yield nearly identical spectra. This is consistent with the selection rules for the hh and lh excitonic transitions for a GaAs(001) thin film under a biaxial stress in which the stress tensor σ has equal orthogonal components, $\sigma_\parallel = \sigma_\perp$. Under a biaxial tensile stress the preferential direction for the quantization of the hole angular momentum m_j is along $\langle 001 \rangle$, emission along this direction is unpolarized in the (001) surface plane as observed, and the lh exciton (identified as peak P_1) is the lowest energy transition.[1,2]

The hh and lh excitonic peak positions from the fits of Fig. 1 are shown in Fig. 2 for the various mesa sizes. The stress-induced lh-to-hh energy splitting reduces from 13.4 meV for the largest mesa (1 mm) to 3.4 meV for the smallest mesa (10 μm). For a biaxial stress in GaAs, the hh-to-lh energy splitting increases at a rate of ~ 6.2 meV/kbar.[1,11,12] The bottom of Fig. 2 shows that the magnitude of the stress

reduces from ~ 2.2 kbar for the 1 mm mesa to 0.5 kbar for the 10 μm mesa. This result is consistent with the PL measurements of Lingunis and co-workers,[3] which showed a similar stress reduction for a 10 μm mesa that was 1 μm thick.

B. Temperature dependence of CL spectra

A series of spectra for the electron beam positioned at the center of the 1 mm mesa is shown in Fig. 3. As the temperature T is increased, the intensity of peak P_2 increases according to the expression $S_2/S_1 = I_{osc} \exp(-\Delta E/kT)$, where, S_1 and S_2 are the integrated intensities of peaks P_1 and P_2, ΔE is the magnitude of the energy splitting between P_1 and P_2, I_{osc} is the hh-to-lh oscillator strength, and k is Boltzmann's constant.[1,2] An Arrhenius plot is shown as an inset to Fig. 3. The linear fit yields $\Delta E = 12.4$ meV and $I_{osc} = 2.1$, which is close to the theoretical value of 3. The energy splitting obtained from the decomposition of the spectra shown in Fig. 3 is 13.4 meV and reasonably close to the ΔE obtained from the fits, thus further supporting the validity of the fitting procedure.

We note that the I_{osc} obtained from the fits is only 70% of the expected value of 3. This is likely a result of the self-absorption of cathodoluminescence, as light generated in the GaAs bulk will be reabsorbed during its propagation to the surface. The effect on the shape of the luminescence spectrum $L(h\nu)$, is[14]

$$L(h\nu) = (1-R)L_0(h\nu)\frac{1-e^{-\alpha t}}{\alpha t}, \quad (1)$$

Tang *et al.*

where R is the reflectivity of the exit surface, $L_0(h\nu)$ is the luminescence intensity that would be measured without self-absorption and surface reflection, α is the absorption coefficient of the sample, and t is the thickness of the sample. Since P_1 has a lower energy than P_2, the effect of self-absorption for P_1 is markedly reduced compared to that for P_2, since both components are close to the absorption edge. The intensity of higher-energy peak P_2 is reduced by a factor of $(1-e^{-\alpha t})/\alpha t$, which is ~0.63 for 1-$\mu$m-thick GaAs ($\alpha \sim 10^4$ cm^{-1} just above the absorption edge).[14] After taking this correction into account the value for I_{osc} has an upper limit of 3.3, and is closer to the theoretical value of 3.

C. Spatial variation of stress tensor

Further investigation shows that stress on a 10 μm mesa evaluated from the peak positions does not vary significantly with location, although stress on a 25 μm mesa has a slight variation throughout the mesa. It is widely accepted that in the vicinity of edge, the mismatched lattice is free to relax,[4,10] resulting in a stress relief in direction perpendicular to the edge. Several analytical and numerical models have been proposed in studying the stress of heteroepitaxial layer.[15–18] The existence of biaxial stress has been established at the centers of all mesas, and the presence of the mesa edge will affect the stress in the vicinity of the mesa edge. Previously, we have shown that near microcracks the GaAs film is subject to uniaxial stress which transforms to biaxial stress for regions greater than ~15 μm away from the cracks.[1] A similar effect should also occur near the mesa edges, where the stress tensor is also free to relax along the direction normal to the edge, resulting in an approximate uniaxial stress. We can describe this stress reduction by introducing a parameter L_D, the decay length of stress relief and the pattern half-width W. The stress component $\sigma_\perp$ as a function of the distance from the center can be expressed using the following bimetal thermostat model:[18]

$$\sigma_\perp(x) = \sigma_m\left(1 - \frac{\cosh(x/L_D)}{\cosh(W/L_D)}\right) + \sigma_0, \qquad (2)$$

where x is the distance from the center, σ_m is the maximum stress reduction at the edge, and σ_0 is the residual stress remaining at the edge. When the size of pattern is much larger than L_D, the effect of the edge on stress relief is very small and the biaxial stress at the center region is independent of the size; however, if the size of mesa is comparable to L_D, the edge becomes an important source of stress relief, the stress should strongly depend on the size of mesa.

Previous studies on the effect of stress on band structure gave the relation between the transition energies and the internal stress tensor.[11,12] Briefly, the relationship between the stress tensor components, $\sigma_\parallel$ and $\sigma_\perp$, and the energy positions of the strain split peaks can be found by determining the resulting strain tensor ϵ_{km} from the elastic constant tensor C_{ijkm}, using the generalized Hooke's law formalism (i.e., $\sigma_{ij} = C_{ijkm}\epsilon_{km}$) and diagonalizing the orbital strain Hamiltonian to find the energy eigenvalues.[9,11,12] The result for the special case of having two orthogonal in-plane stress components $\sigma_\parallel$ and $\sigma_\perp$ (both defined with respect to $\langle 110 \rangle$ direc-

tions), a peeling stress (transverse normal and parallel to the growth direction)[18] σ_z, and a shear stress[18] τ in GaAs, is

$$E_\pm = E(0) - A(\sigma_\parallel + \sigma_\perp + \sigma_z) \pm \{B^2(\sigma_\parallel + \sigma_\perp - 2\sigma_z)^2 + C^2[(\sigma_\parallel - \sigma_\perp)^2 + 4\tau^2]\}^{1/2}, \qquad (3)$$

where $E_\pm$ are the stress-split transition energies, $E(0)$ is the transition energy in absence of stress. The shear term τ is defined with respect to the $\langle 110 \rangle$ directions and, when present, results in tangential components of opposing forces along the GaAs/Si interface and GaAs surface. The constants A, B, and C are related to deformation potentials of GaAs.[9] Using the data from the piezoelectroreflectance measurement of Pollak and Cardona,[11] we have

$$A = a(S_{11} + 2S_{12}) = 3.8 \text{ meV/kbar},$$

$$B = \tfrac{1}{2}b(S_{11} - S_{12}) = 1.55 \text{ meV/kbar},$$

and

$$C = \tfrac{1}{4}dS_{44} = 2.31 \text{ meV/kbar},$$

where a is the hydrostatic pressure deformation potential, b and d are uniaxial deformation potentials associated with strains of tetragonal and rhombohedral symmetries, and S_{ij} are elastic compliance constants which form the inverse of the elastic constant tensor. Given the energies of the two strain-split excitonic transitions, we can determine the local stress tensor based on this equation, for regions sufficiently far from the mesa edges, where σ_z and τ are both expected to approach zero (as discussed in Ref. 18). For biaxial stress case, $\sigma_\parallel = \sigma_\perp$, splitting is $4B\sigma$, while under uniaxial stress splitting becomes $2(B^2 + C^2)^{1/2}\sigma_\parallel$, under the usual assumption of $\sigma_z = \tau = 0$.[1,2]

The scanning capability of the SEM allows us to investigate μm-scale spatial variations. To further investigate the stress distribution on the mesa and confirm the model of Eq. (2), spectra were taken, for mesa sizes ranging from 10 to 1000 μm, as a function of the distance from the edge of mesa by fixing the electron beam at positions along the path parallel to [1$\bar{1}$0] from the edge to the center. The experimental results indicate that as the electron beam scans from the center toward the edge, the position of the exciton peaks shifts to higher energies and the splitting of P_1 and P_2 exciton peaks is reduced. Figure 4 shows a stack plot of local polarized CL spectra taken as a function of distance from the [110] edge of the 250 μm square mesa. The resulting positions of peaks P_1 and P_2 obtained from the fits for the 250 μm mesa are plotted in Fig. 5. A distinct increase in the polarization anisotropy for the polarizer orientations used to detect emissions with $\mathbf{E} \perp [110]$ and $\mathbf{E} \parallel [110]$ is observed as the beam is positioned close to the mesa edge. For a pure uniaxial tensile stress along [110], the preferential direction for quantization of the hole angular momentum m_j is along [110], and the lowest energy transition (P_1) has primarily a hh character.[1,2,11,12] Thus, regions of pure biaxial and pure uniaxial stress must have a reversed energy order for the hh and lh exciton transitions. The hh excitonic transition for pure uniaxial tensile stress results in emission which is linearly polarized perpendicular to the mesa edge.[1,2] In Fig. 4 for $x = 0.4$ μm, the hh-to-lh peak intensity ratio changes
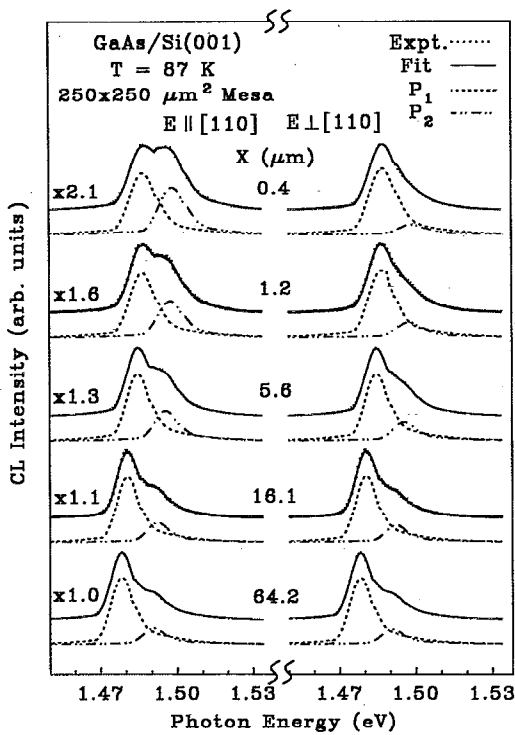
FIG. 4. Local polarized CL spectra as a function of the distance from the edge of the 250 μm mesa for the polarizer detection orientations of $E\perp[110]$ and $E\|[110]$. The decomposition of the luminescence line shape into two components (labeled as P_1 and P_2) resulting from the strain-induced splitting of the top valence bands is shown. The overall fit to the data is indicated by a solid line running through the data. The factors used to scale spectra for $E\|[110]$ detection relative to the spectra for $E\perp[110]$ detection are shown.

from 6.4 to 1.3 as the polarizer is rotated from the $E\perp[110]$ to $E\|[110]$ detection orientations. This confirms the strong uniaxial character of the stress at the mesa edge.

Quantitatively, we can deduce from the positions of the excitonic transitions, the stress components along two orthogonal $\langle 110 \rangle$ directions, $\sigma_\perp$ and $\sigma_\|$, by utilizing Eq. (3) without including shear and peeling stress terms (i.e., $\sigma_z = \tau = 0$).
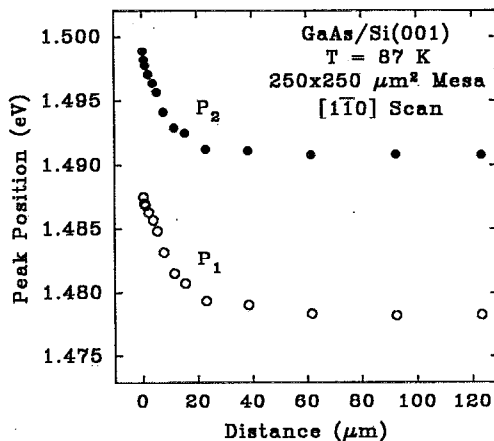

FIG. 5. Energy positions of the strain split peaks P_1 and P_2 as a function of the distance from the [110]-oriented edge of the 250 μm mesa.
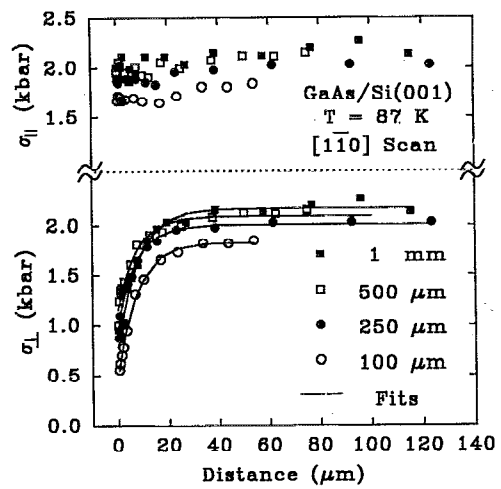

FIG. 6. The calculated stress components $\sigma_\|$ and $\sigma_\perp$, using Eq. (3) and the condition $\sigma_z = \tau = 0$, as a function of the distance from the edge for the mesa sizes indicated. The fits to the data using the model of Eq. (2) are indicated by the solid lines in the figure.

The energy of the excitonic transition for zero applied stress $E(0)$ was determined by examining the luminescence from MOCVD-grown GaAs on GaAs(001) grown under the same conditions. A result of $E(0) = 1.506$ eV was found at 87 K. Figure 6 shows the stress components $\sigma_\|$ and $\sigma_\perp$ as the function of distance for different mesa sizes derived from the results of Fig. 5 and data for the other mesas not shown here. The results of Fig. 6 show that $\sigma_\|$ does not vary significantly with distance, although the stress increases as the mesa size increases. Because of the reduction of $\sigma_\perp$, the character of stress changes from biaxial at the center to nearly uniaxial at the edge, as also confirmed by the polarization anisotropy of hh excitonic transition near the edges of all mesas. For $x > \sim 15$ μm the lh and hh transitions have the same intensities for the two polarization directions for all mesas studied here, which is consistent with the selection rules for biaxial stress as previously discussed. It can be seen that the stress reduction behavior for different sizes are very similar. The fitting of $\sigma_\perp(x)$ with Eq. (2) is shown with lines through the data of Fig. 6.

The results of the fits showing L_D versus the mesa size are shown in Fig. 7. The decay length L_D is seen to increase from 3.9 to 7.8 μm as the mesa size increases from 25 to 100 μm, and, after which, no significant change in L_D is found. It is evident, using Eq. (2), that L_D decreases for mesas less than 100 μm because the size of the mesa becomes comparable to L_D, and all four edges of the square will interact in relieving the stress. For the 10 μm mesa, no detectable decay in the stress was observed as the beam was positioned from the mesa edge, indicating a completely homogeneous stress as reported in Sec. III A. The residual tensile stress remaining at the $x = 0$ edge, $\sigma_\perp(0)$, is seen to fluctuate between 0.5 and 1 kbar in Fig. 6. An increase in $\sigma_\perp(0)$ is seen for mesa sizes greater than 100 μm. The experimentally determined values of $\sigma_\perp(0)$ and $\sigma_\|(0)$ are shown in Fig. 7 (labeled as exp.) as a function of the mesa sizes.

An elastic finite-element (FE) analysis was performed on

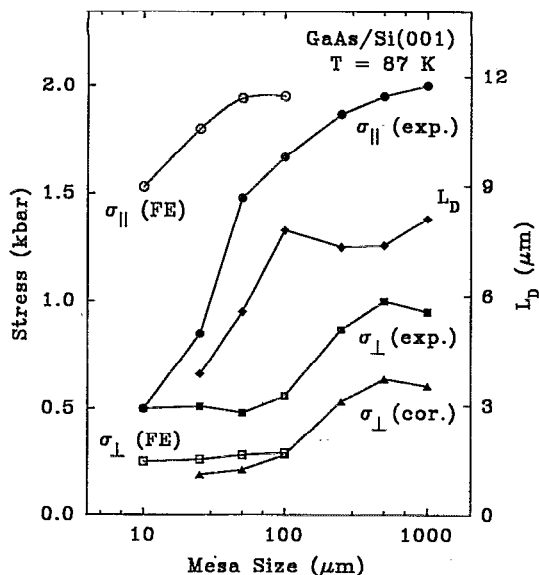FIG. 7. The decay length L_D, the parallel stress $\sigma_\parallel$, and the residual stress $\sigma_\perp$ as a function of the mesa size using solutions to the bimetal decay model and the orbital-strain Hamiltonian, as described by Eqs. (2) and (3), respectively. The values for $\sigma_\parallel$ (exp.) and $\sigma_\perp$ (exp.) at the mesa edges ($x=0$) are indicated by ● and ■, respectively, assuming $\sigma_z = \tau = 0$. When incorporating shear and peeling stresses (based on the model of Suhir in Ref. 18) in the calculation for $\sigma_\perp$ at $x=0$, the corrected values $\sigma_\perp$ (cor.) are indicated as ▲ in the figure. ○ and □ represent the results of a finite-element (FE) analysis for $\sigma_\parallel$ and $\sigma_\perp$.
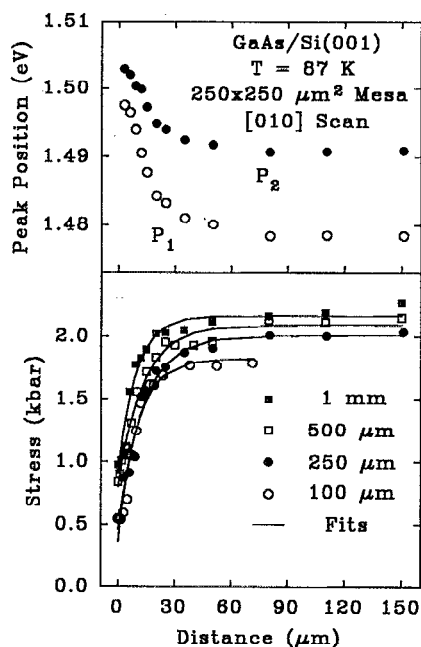

FIG. 8. The biaxial stress, calculated using Eq. (3) and the condition $\sigma_z = \tau = 0$, as a function of the distance from a corner along [010]. The solid lines are the results of fits using the model of Eq. (2). The energy positions of peaks P_1 and P_2 are shown as a function of the distance from the mesa corner for the case of the 250 μm mesa.

these GaAs mesas. The computational details of this analysis have been previously described.[9,15] Briefly, the substrate and the epilayer are assumed stress free at the growth temperature ~800 K and thermal stresses were calculated at 87 K using the SAP90™ finite-element code;[9,15] the Young's modulus, Poisson's ratio, and thermal-expansion coefficient used in the calculation were 860 kbar, 0.31, and 5.8×10^{-6} K^{-1} for GaAs and 1300 kbar, 0.28, and 2.6×10^{-6} K^{-1} for Si, respectively. Four different width-to-thickness aspect ratios were examined (10, 20, 50, and 100) and the maximum stresses [$\sigma_\perp(0)$ and $\sigma_\parallel(0)$] calculated are shown in Fig. 7. The maximum stresses were found to exist near the GaAs-Si interface for $x=0$, where the strain in the GaAs film will be the largest. The corresponding stresses near the GaAs surface, for $x=0$, were found to be close to zero. Since CL will sample the entire 1 μm thickness of the film, we would expect to measure intermediate values for $\sigma_\parallel(0)$ (between 0 and the maximum from the FE analysis), which is the case shown in Fig. 7. The FE stress calculations and the stress values obtain from P_1 and P_2 positions using Eq. (3) show, however, a good qualitative agreement, as $\sigma_\perp(0)$ and $\sigma_\parallel(0)$ are both seen to increase with increasing mesa size.

The stress relief at the corner regions can be examined in a similar fashion. The electron beam was positioned along the line parallel to [010] from the corner toward the center of the mesas, which is at a 45° direction with respect to the edge. The stress is biaxial because of the symmetry and the spectral lineshapes were independent of the polarizer orientation. The hh-to-lh energy splitting approaches zero as the corner was approached (as shown, e.g., for the 250 μm mesa

case in Fig. 8), indicating stress relief in the vicinity of the corner. Using Eqs. (2) and (3), with $\sigma_\parallel = \sigma_\perp$ for the case of biaxial stress, the stress values and decay lengths have been determined in a manner similar to the case for uniaxial stress described above. The L_D value obtained by fitting the stress with Eq. (2) for mesas greater than 100 μm is ~11.7 μm, which is very close to $\sqrt{2}$ times that previously obtained for the uniaxial stress decay near the edge. The data of Fig. 8 show that residual tensile stress remains even at the corners.

Previous studies attempted to show that it was possible to achieve complete stress relief of one component ($\sigma_\perp = 0$) at an edge or microcrack and both components ($\sigma_\parallel = \sigma_\perp = 0$) at a corner.[1,4,10] Recently, a CL study has shown that a compressive stress may occur at the edge. Lingunis and co-workers have shown that, near edges of selectively grown GaAs stripes possessing various width-to-thickness ratios, a small compressive stress of ~−0.5 kbar was observed.[3] The results of Fig. 7 [for $\sigma_\perp$ (exp.)] show that the stress near the edges and corners is still tensile and ranges from 0.5 to 1 kbar. There are additional types of edge-related stresses, as indicated in Eq. (3) by the presence of peeling σ_z and shear τ terms. These terms can generally be comparable in magnitude to $\sigma_\parallel$ and $\sigma_\perp$ for thermally mismatched thin films, as indicated in the calculations of Suhir,[18] who showed that a tensile peeling stress and nonzero shear stress can exist near the edge a thin film as a result of a nonzero stress in the growth direction.[18] This tensile peeling stress would tend to cause the positions of P_1 and P_2 to move in the same direction as a tensile stress for $\sigma_\perp$, by considering the hydrostatic deformation term in Eq. (3). We have calculated the general dependence for $\sigma_z(x)$ and $\tau(x)$ using Suhir's bimetal ther-
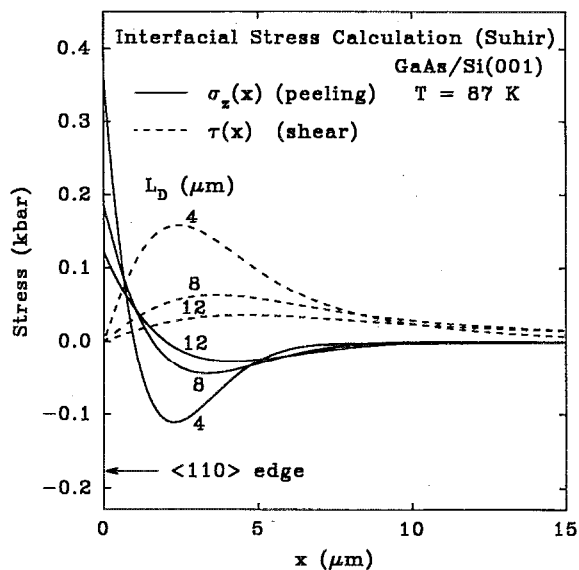
FIG. 9. Calculations of Interfacial peeling (solid line) and shear stress (dashed line) as a function of distance from a ⟨110⟩ mesa edge (for mesa sizes $W \gg L_D$) using the bimetal thermostat model of Suhir (Ref. 18) for our case of GaAs/Si(001) at $T = 87$ K.
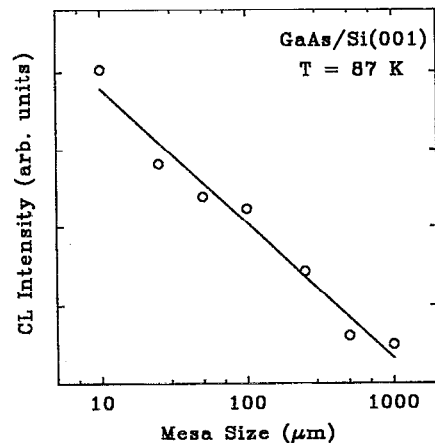

FIG. 10. The integrated cathodoluminescence intensity as a function of the mesa size. The solid line indicates a linear fit and shows a logarithmic dependence of the CL intensity on the mesa size.

mostat model,[18] using the same elastic parameters of Young's modulus, Poisson's ratio, and thermal-expansion coefficient that were used in our finite-element analysis previously described; the results are shown in Fig. 9 for our case of GaAs/Si(001). The results for three different values of L_D (4, 8, and 12 μm) are shown in Fig. 9, and these results are valid for mesa sizes $W \gg L_D$; for smaller sizes the effects of opposite edges will affect this calculation. For example, from Fig. 9, the maximum values for shear and peeling stresses are 0.063 and 0.185 kbar, respectively, for $L_D = 8$ μm. Using the maximum values of $\sigma_z(x)$ and $\tau(x)$ from the bimetal model, we have obtained corrected values for $\sigma_\perp$ (cor.) at $x = 0$; these corrected values are shown in Fig. 7 (solid triangles). Appropriate values for L_D (as shown in Fig. 7) were used in the calculation of $\sigma_\perp$ (cor.) for each mesa size. As a result of inclusion of peeling and shear terms, the values for $\sigma_\perp$ are seen to range from about 0.2 to 0.6 kbar for mesa sizes increasing from 25 to 1000 μm. These $\sigma_\perp$ (cor.) data more closely correlate with that of the FE analysis, as observed in Fig. 7. Therefore, we conclude that the accuracy of $\sigma_\perp$ near mesa edges can be enhanced by inclusion of σ_z and τ, the relative contributions of $\sigma_\perp$, $\sigma_\parallel$, σ_z, and τ in close proximity to mesa edges are estimated by utilizing the solutions of Eq. (3), the bimetal thermostat model of Suhir,[18] and the polarized CL data of the strain-split excitonic peak positions. We note that the magnitude of the stress near the edges is uncertain due to the ~0.5 μm minority-carrier diffusion length. The approximately exponentially decay [see Eq. (2) for small x] of stress near the edge results in an exponential increase in the bandgap [from Eq. (3)] as the edge is approached. This gradient in the band gap could induce excess electrons and holes to drift away from the edge or corners, to a region of lower band gap, resulting in an effective increase in measured $\sigma_\perp$ values. However, our lack of knowledge of the band bending in the vicinity of the mesa edges and surface precludes any quantitative assessment of this effect.

D. Luminescence efficiency and dislocation generation

The selective growth of thin films on reduced areas is known to enhance the optical and structural quality of the film when the epilayer and substrate are lattice mismatched.[3,19] Yamaguchi et al.[20] recently showed a reduction in the dislocation density, using the etch-pit method, for MOCVD selectively grown GaAs on Si. It was argued that the reduction in thermal stress present for the smaller pattern sizes would lead to a reduction in the stress-induced dislocation density, and a linear correlation between stress and dislocation density was established by these authors. The integrated CL intensity is shown versus the mesa size in Fig. 10. The CL intensity is found to decrease nearly logarithmically with the mesa size, thus indicating an increase in the structural quality of the GaAs films for smaller mesa sizes. These results do, therefore, confirm that stress induced dislocations, whether thermal or lattice mismatch in nature, can be reduced through selective growth on reduced areas.

E. Linearly polarized CL imaging

In order to assess the homogeneity of the optical quality of the entire mesa region, it is necessary to employ the CL imaging capability. The optical quality can vary from point to point on the GaAs mesa as a result of dislocations and stacking faults resulting from the large lattice mismatch between Si and GaAs. Imperfections in the etching of the SiO_2 mask before GaAs growth and its chemical removal after growth can lead to deviations from a perfect square mesa pattern, and subsequently lead to inhomogeneities in thermal stress. The microcracks resulting from the thermal stress will occur when the mesa size exceeds a critical value, and CL imaging can be used to determine this. A useful nondestructive approach to obtain immediate feedback on the quality of device structure and its degree of homogeneity is to perform
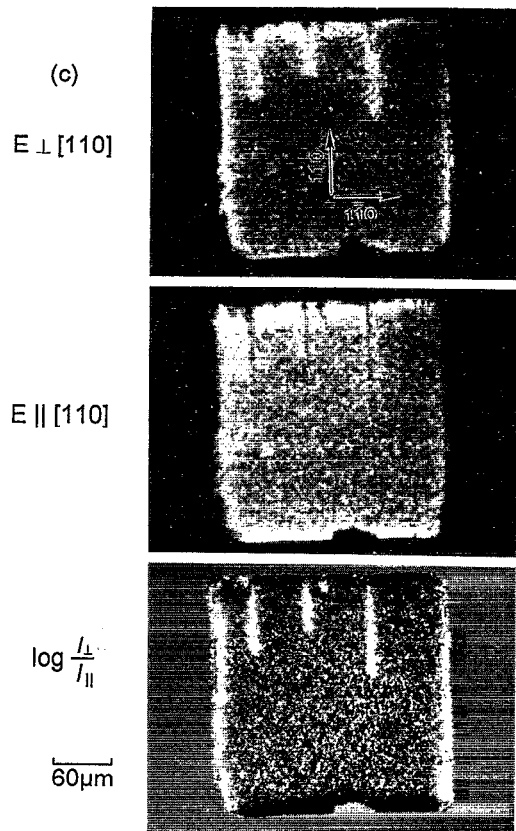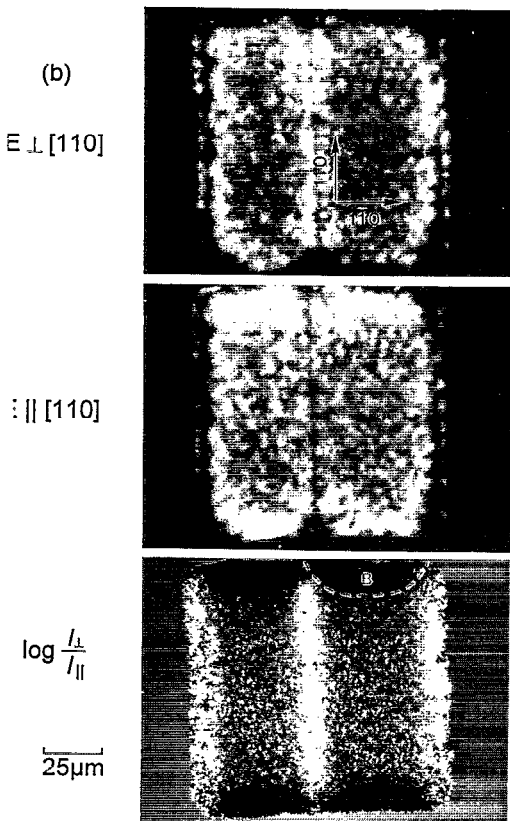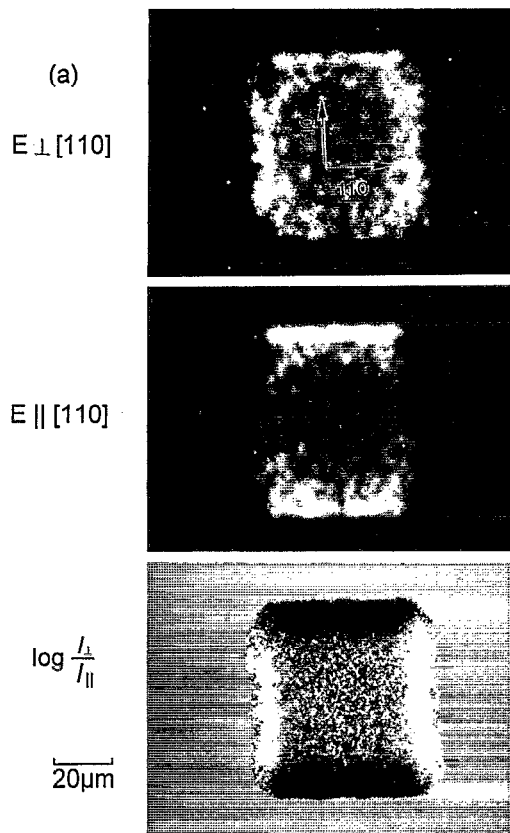
(a)

E ⊥ [110]

E ∥ [110]

$\log \dfrac{I_\perp}{I_\parallel}$

20μm

(b)

E ⊥ [110]

E ∥ [110]

$\log \dfrac{I_\perp}{I_\parallel}$

25μm

(c)

E ⊥ [110]

E ∥ [110]

$\log \dfrac{I_\perp}{I_\parallel}$

60μm

FIG. 11. Linearly polarized CL images for mesa sizes of (a) 50, (b) 100, and (c) 250 μm. For each mesa, three images showing the polarization detection conditions of E⊥[110], E∥[110], and $\log(I_\perp/I_\parallel)$ are indicated. The shape of a biaxial stress boundary contour, for example, can be identified as a dashed line near the region labeled B in (b).

CL imaging. In particular polarized CL imaging can enable the immediate identification of regions which deviate from an ideal biaxial stress. Figure 11 shows polarized monochromatic CL images of 50, 100, and 250 μm mesas. Photon energies of 1.494 eV (50 μm mesa) and 1.487 eV (100 and 250 μm mesas) were detected in the monochromatic CL imaging. The photon energies were chosen so as to correspond to the peak of the hh excitonic transition that occurs near the edges of the mesas. The images were taken with the polarizer rotated to detect emission of light with E⊥[110] and E∥[110]

detection orientations, as indicated in the figure. When the polarizer is oriented so as to detect emission with $E \perp [110]$, the regions near the square mesa edges which are parallel and perpendicular to [110] become bright and dark, respectively. This is a result of the linearly polarized property of excitonic emission associated with the hh wave function as discussed in Sec. III C. Also, in order to emphasize the regions which show a polarization dependence, the ratio of the images is displayed. The pixels in the ratio images at a (x,y) position are represented as $\log[I_\perp(x,y)/I_\parallel(x,y)]$, where $I_\perp(x,y)$ and $I_\parallel(x,y)$ are the pixel intensities under $E \perp [110]$ and $E \parallel [110]$ detection orientations, normalized to a 256 level grey scale. Regions of uniform bright and dark contrast indicate deviations from biaxial stress and occur near regions of uniaxial stress. For mesa sizes greater than or equal to 100 μm, microcracks were found to run parallel to [110] as can be seen in Figs. 11(b) and 11(c). The polarization dependence of the luminescence near the microcracks is similar to that near the mesa edges, and the microcracks were previously found to exhibit a nearly uniaxial stress dependence.[1] The shape of the biaxial stress boundary contour can be seen near the regions in Fig. 11(b) labeled B. Figure 11(c) shows results from a nonideal 250 μm mesa containing microcracks and defects near the meas edges. Again, the bright and dark regions pinpoint regions of stress relief. The microcracks do not necessarily propagate through the entire mesa as seen in Fig. 11(c). Thus, polarized CL image can sensitively identify small deviations from pure biaxial stress resulting from defects.

IV. CONCLUSION

In conclusion, we have examined the variation of stress tensor in selective-area MOCVD-grown GaAs on Si substrate by using the polarized CL technique. Patterns with smaller dimensions show better optical quality, indicating a reduction in the thermal-stress-induced dislocation density. The biaxial stress is found to decrease for small mesa sizes, and a stress reduction near the edges and corners is found to be modeled well with a bimetal thin-film model. A residual stress (0.5–1.0 kbar) exists on the corner. The CL results show that (i) the decay length of stress relief near a pattern edge increases with increasing mesa size, (ii) the maximum biaxial stress and residual stress near the mesa edges increase with increasing pattern size, and (iii) the luminescence efficiency of the film decreases with increasing pattern size. The residual stress near the mesa edges is generally comprised of transverse normal $\sigma_\perp$, shear τ, and peeling σ_z terms whose relative contributions can be determined from the polarized CL strain-split peak positions, solutions to the orbital-strain Hamiltonian, and bimetal thermostat model of Ref. 18. A

finite-element analysis showed that $\sigma_\parallel$ and $\sigma_\perp$ increase with increasing mesa size in qualitative agreement with the data. The selective-area growth method improves the quality of thermally mismatch epilayer materials and helps to reduce the thermal stress on the heteroepitaxial layer. Polarized CL imaging is observed to be sensitive to local deviations from biaxial stress and can be used to map the boundaries of stress contours near mesa edges and defects.

ACKNOWLEDGMENTS

[1] D. H. Rich, A. Ksendzov, R. W. Terhune, F. J. Grunthaner, B. A. Wilson, H. Shen, M. Dutta, S. M. Vernon, and T. M. Dixon, Phys. Rev. B 43, 6836 (1991).

[2] H. Shen, M. Dutta, D. W. Eckart, K. A. Jones, S. M. Vernon, and T. M. Dixon, J. Appl. Phys. 68, 369 (1990).

[3] E. H. Lingunis, N. M. Haegel, and N. H. Karam, Solid State Commun. 76, 303 (1990).

[4] S. Zemon, C. Jagannath, E. S. Koteles, S. K. Shastry, P. Norris, G. Lambert, A. N. M. Choudhury, and C. A. Armiento, in Gallium Arsenide and Related Compounds—1986, Proceedings of the 13th International Symposium, edited by W. T. Lindley, IOP Conf. Proc. No. 83 (Institute of Physics and Physical Society, Bristol, 1987), p. 141.

[5] S. Zemon, S. K. Shastry, P. Norris, C. Jagannath, and G. Lambert, Solid State Commun. 58, 457 (1986).

[6] A. Freundlich, H. Kamada, G. Neu, and B. Gil, Phys. Rev. B 40, 1652 (1989).

[7] T. Kanata, H. Suzawa, M. Matsunaga, H. Takakura, Y. Hamakawa, H. Kato, and T. Nishino, Phys. Rev. B 41, 2936 (1990).

[8] M. Dutta, H. Shen, S. M. Vernon, and T. M. Dixon, Appl. Phys. Lett. 57, 1775 (1990).

[9] E. H. Lingunis, N. M. Haegel, and N. H. Karam, J. Appl. Phys. 74, 2779 (1993).

[10] B. G. Yacobi, C. Jagannath, S. Zemon, and P. Sheldon, Appl. Phys. Lett. 51, 2236 (1987); 52, 555 (1988); J. Cryst. Growth 95, 249 (1989).

[11] F. H. Pollak and M. Cardona, Phys. Rev. 172, 816 (1968); F. H. Pollak, Semiconductors and Semimetals, edited by R. K. Willardson and A. C. Beer (Wiley, New York, 1990), Vol. 32, pp. 17–53.

[12] M. Chandrasekhar and F. H. Pollak, Phys. Rev. B 15, 2127 (1977).

[13] H. Kroemer, J. Cryst. Growth 81, 193 (1987).

[14] B. G. Yacobi and D. B. Holt, in Cathodoluminescence Microscopy of Inorganic Solids (Plenum, New York, 1990), p. 39; J. I. Pankove, Optical Processes in Semiconductors (Dover, New York, 1971).

[15] E. H. Lingunis, N. M. Haegel, and N. H. Karam, Appl. Phys. Lett. 59, 3428 (1991).

[16] I. A. Blech and A. A. Levi, ASME J. Appl. Mech. 48, 442 (1981).

[17] S. M. Hu, J. Appl. Phys. 50, 4661 (1979).

[18] E. Suhir, ASME J. Appl. Mech. 53, 657 (1986); 55, 143 (1988); 56, 595 (1989).

[19] N. H. Karam, V. Haven, S. M. Vernon, N. El-Masry, E. H. Lingunis, and N. M. Haegel, J. Cryst. Growth 107, 129 (1991).

[20] M. Yamaguchi, M. Tachikawa, M. Sugo, S. Kondo, and Y. Itoh, Appl. Phys. Lett. 56, 27 (1990).